Hindawi Publishing Corporation
International Journal of Geophysics
Volume 2011, Article ID 496123, 19 pages
doi:10.1155/2011/496123

Research Article

Site Assessment of Multiple-Sensor Approaches for Buried Utility Detection

Alexander C. D. Royal,[1] Phil R. Atkins,[2] Michael J. Brennan,[3] David N. Chapman,[1] Huanhuan Chen,[4] Anthony G. Cohn,[4] Kae Y. Foo,[2] Kevin F. Goddard,[5] Russell Hayes,[1] Tong Hao,[1] Paul L. Lewin,[5] Nicole Metje,[1] Jen M. Muggleton,[3] Adham Naji,[6] Giovanni Orlando,[6] Steve R. Pennock,[6] Miles A. Redfern,[6] Adrian J. Saul,[7] Steve G. Swingler,[5] Ping Wang,[5] and Christopher D. F. Rogers[1]

[1] *School of Civil Engineering, University of Birmingham, Birmingham B15 2TT, UK*
[2] *School of Electronic, Electrical and Computer Engineering, University of Birmingham, Birmingham B15 2TT, UK*
[3] *Institute of Sound and Vibration Research, University of Southampton, Southampton SO17 1BJ, UK*
[4] *School of Computing, University of Leeds, Leeds LS2 9JT, UK*
[5] *School of Electronics and Computer Science, University of Southampton, Southampton SO17 1BJ, UK*
[6] *Department of Electronic and Electrical Engineering, University of Bath, Bath BA2 7AY, UK*
[7] *Department of Civil and Structural Engineering, University of Sheffield, Sheffield S10 2TN, UK*

Correspondence should be addressed to Alexander C. D. Royal, a.c.royal@bham.ac.uk

Received 12 February 2011; Accepted 15 April 2011

Academic Editor: Erica Utsi

The successful operation of buried infrastructure within urban environments is fundamental to the conservation of modern living standards. Open-cut methods are predominantly used, in preference to trenchless technology, to effect a repair, replace or install a new section of the network. This is, in part, due to the inability to determine the position of all utilities below the carriageway, making open-cut methods desirable in terms of dealing with uncertainty since the buried infrastructure is progressively exposed during excavation. However, open-cut methods damage the carriageway and disrupt society's functions. This paper describes the progress of a research project that aims to develop a multi-sensor geophysical platform that can improve the probability of complete detection of the infrastructure buried beneath the carriageway. The multi-sensor platform is being developed in conjunction with a knowledge-based system that aims to provide information on how the properties of the ground might affect the sensing technologies being deployed. The fusion of data sources (sensor data and utilities record data) is also being researched to maximize the probability of location. This paper describes the outcome of the initial phase of testing along with the development of the knowledge-based system and the fusing of data to produce utility maps.

1. Introduction

The preservation of buried infrastructure within the urban landscape is of fundamental importance if modern living is to be maintained. Failure to maintain the buried infrastructure can rapidly result in breakdown of utility service provision; yet traditional open-cut methods used to repair and replace the buried utilities are inherently disruptive to society's functions and damaging to the carriageway (beneath which the utilities are commonly buried), and potentially the buried infrastructure itself. A recent UK study estimated that street works cost the UK £7bn in lost revenues annually; comprising £5.5bn in social costs and £1.5bn in direct damages [1]. Open-cut practices deployed within the carriageway constitute a significant proportion of this work, and hence cost. Trenchless technology could be used in place of open-cut methods when installing or repairing the buried infrastructure, although concerns over the risk of damaging existing adjacent utilities have limited the uptake of these techniques (particularly those that excavate, displace,

or otherwise disturb the ground). These risks partially stem from the inability to precisely locate all buried utilities below the carriageway without some form of proving excavation. Mapping the Underworld (MTU) is a research initiative that aims to research and develop the tools necessary to locate all utilities below the carriageway and record their position, thereby promoting the use of trenchless technology. One of the MTU research projects focuses on developing a prototype multisensor platform that can be used to improve the probability of complete detection of all buried utilities below the carriageway.

2. Development of MTU Multisensor Device

The MTU initiative is an umbrella for several EPSRC-funded projects that collectively aim to research and develop the tools necessary to locate, position, and electronically record the buried utilities, in the context of UK practices. Projects include the development of resonant RFID tags, which can be affixed to new utilities, or retrofitted to existing utilities during periods of maintenance and repair, that improve detection rate of the buried utilities when using Ground Penetrating Radar (GPR) [2]; the development of surveying techniques to permit the accurate positioning of utilities in heavily built up urban environments (so-called "urban canyons" where traditional GPS can struggle to operate); the development of a database that integrates existing electronic and paper records denoting utilities locations across the utilities industry [3]. The MTU initiative also includes the research and development of a multisensor device, a platform that will employ four geophysical location technologies previously identified in a feasibility study [4] as being potentially complementary and which, when intelligently combined, should improve the probability of utility detection. The four sensing technologies comprise GPR, vibro-acoustics, low-frequency electromagnetic fields (LFEM), and passive magnetic fields (PMF).

The creation of the MTU multisensor device is a novel undertaking [4]: the authors are not aware of a platform previously created using these four sensing technologies, and indeed a number of the sensing technologies are being developed from first principles for this project. However, the construction of the multisensor device in itself does not represent the sea change that the MTU initiative aims to achieve; prototype multisensor devices have been created in the past and utility location companies may also deploy multiple geophysical detection technologies sequentially on a site when the situation demands it. Empirical experiences from the utility location industry would suggest the deployment of a geophysical device, or a suite of devices, without prior knowledge of the site in question makes detection of all utilities difficult in all but the simplest of ground conditions and utility layouts. The ground-breaking aspect of this MTU project arises from how the device is to be deployed and how the data are analysed (Figure 1). The project considers two additional streams of information that could potentially be used to enhance the data acquired by the multisensor device: the ground conditions encountered on site and the existing electronic utility location records. This information will be incorporated into the surveying protocols developed for the prototype device to optimise deployment and to increase the probability that all buried utilities are located.

It is well understood that the ground conditions can have a significant effect upon the performance of the geophysical location technologies employed to find the buried utilities, therefore in conjunction with the multisensor device, research is being undertaken into both the relationship between the geotechnical properties and corresponding geophysical properties of various soils, and changes in geophysical properties for various soils with the seasons (or more precisely recent weather conditions) to provide the foundations for the development of a soil evaluation knowledge-based system. This will be used to inform the surveyor of potential problems for one or more of the sensing technologies on the site and facilitate the optimisation of the deployment of the device on the site. In addition to the focus on ground conditions, research is being undertaken to incorporate existing utility position records into the process. Records tend to exist for utilities buried on a given site (presuming that the utilities present do not predate the keeping of modern records), and whilst these records are neither always accurate in the locations they report nor complete, they do provide an indication of what should be encountered when surveying the site. Research undertaken in the VISTA project [3] has led to the development of a common database for the utility sector and new research is underway to use data held on the VISTA database to improve surveying practices. Not only could the information held on the database act as a primer, giving an indication of what to expect when surveying the site, during the desk study, but it could also be used as a first approximation of layout and fused with the data emanating from the multisensor device to produce a probability map for the layout of the utilities. Such an approach should increase the likelihood of detection. Furthermore, fusing the data together could also highlight discrepancies within the electronic record, thereby facilitating the updating of the records to improve the electronic resource for future use.

The MTU multisensor device project is a four-year research programme funded by the UK's Engineering and Physical Sciences Research Council (EPSRC) and commenced in January 2009. The sensing technologies for the project are all being developed specifically for the project, either from first principles (LFEM and PMF) or as fundamental enhancements of the existing state of the art. By the end of 2010 the majority of the sensing technologies had been developed to a point where testing in field conditions could be undertaken and the results from the initial tests are described herein with the aim of drawing the first raft of important conclusions for those working in this topic area.

2.1. The Sensing Technologies

2.1.1. Ground Penetrating Radar. GPR, reckoned by many to be the mainstay of the shallow geophysical techniques used to detect buried utilities, is being developed for two applications in the MTU project. The first application is a traditional

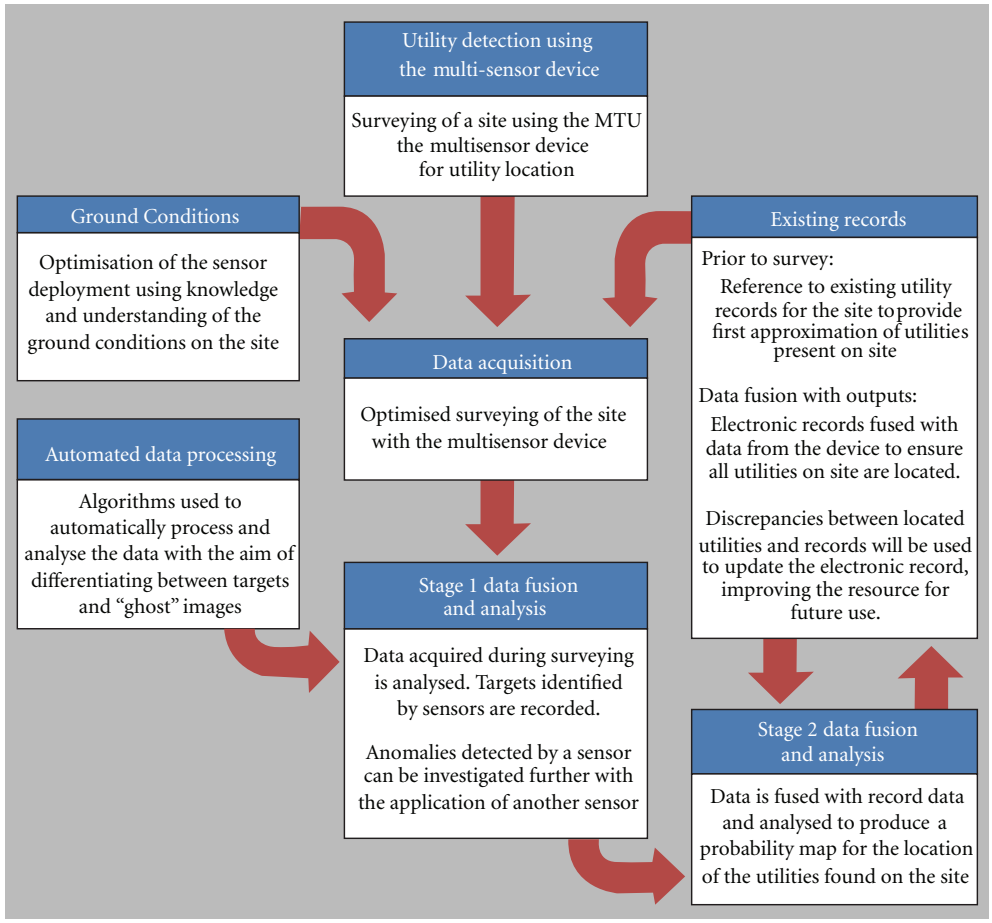

Figure 1: Flow diagram illustrating the principles behind the MTU multisensor device.

surface-mounted GPR sensor, that is, it is configured in "look-down" mode, while the second is an in-pipe GRP sensor that can be equipped with transmitter (Tx) and receiver (Rx) antennas to either "look-out" (by combining the Tx and Rx in the in-pipe device) or "look-through" with the Tx in pipe and the Rx mounted on the surface (Figure 2), or indeed vice versa. The GPR being developed for the project is configured to permit Orthogonal Frequency Division Multiplexing (OFDM; see Figure 3), as results of theoretical modelling suggest that swept frequency GPR (such as OFDM) could improve detection rates [6]. Unlike the other sensing technologies developed for the project, which are predominantly assembled in-house or from components purchased off the shelf, the bespoke components of the GPR have been outsourced for manufacture and its manufacture is only now being finalised. Initial proof testing has therefore been restricted to a commercially available dual frequency pulse-system GPR (250 MHz and 700 MHz) with the aim of determining whether conflicts between the sensing technologies arise when used in conjunction.

2.1.2. Vibro-Acoustics. The outcomes from a prior feasibility study [8] identified that a vibro-acoustic detection system would offer the opportunity to locate buried infrastructure, in particular plastic pipes. Two basic deployment strategies were identified: direct excitation of the utility (via an access point, such as a man hole) and excitation of the ground. A modified system would also have significant potential for use in pipe, although this is not being researched at this stage.

Detection via pipe excitation arose from previous work on leak noise propagation and detection [9–11], indicating that when a leak is present, a significant amount of energy can propagate from the pipe to the surrounding medium at low frequencies. This energy then propagates to the ground surface. Whilst most leaks will not generate enough energy to significantly excite the necessary ground-borne waves, if the fluid in the pipe is excited intentionally, the energy propagation away from the pipe could be exploited to locate underground pipes. The technique is depicted in simplified form in Figure 4, with excitation of either the fluid directly or of the pipe structure. However, it is envisaged that it might be possible to locate buried pipe work by exciting the ground surface in the vicinity of the pipe and detecting the presence of waves scattered from it. When the ground is mechanically excited, waves will propagate away from the excitation point. Depending on the form of excitation, different wave types will be excited in the ground and these waves can be detected, depending of course on the frequency, at ranges of tens of metres. However they will be scattered

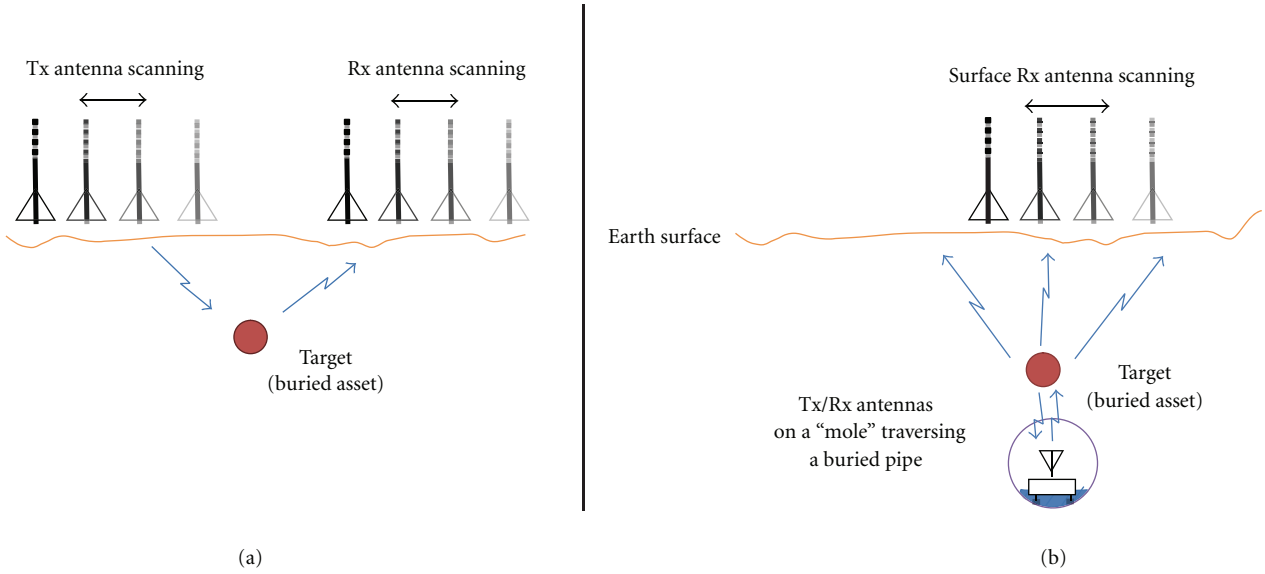

Figure 2: Two GPR applications: (a) traditional look-down mode and (b) look-out or look-through mode (where Tx is the transmitter and Rx the receiver antenna) (images previously published in Royal et al. [5]).

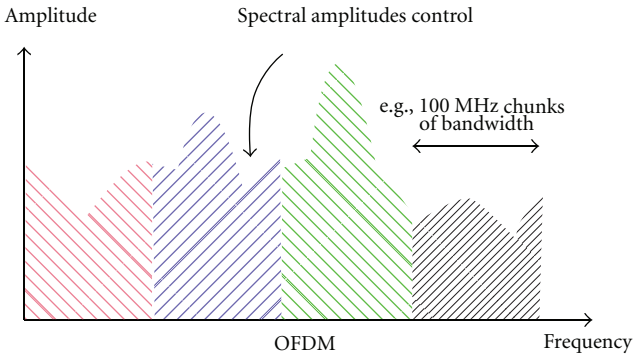

Figure 3: Illustration of Swept Frequency GPR: OFDM.

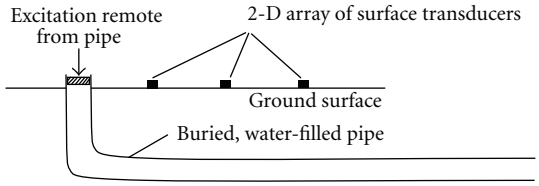

Figure 4: Illustration of pipe detection with vibro-acoustic sensing technology via excitation of water filled pipe (first published in [7]).

by objects, such as pipes, whose mechanical properties are different from the soil, even if the pipes are buried several metres deep. Detection and analysis of the scattered waves would, in principle, allow the pipes to be accurately located. Two possible basic configurations for this technique are shown in Figures 5(a) and 5(b), respectively.

Previous measurements on a dedicated experimental pipe rig [8] demonstrated that the pipe excitation method could be successful in locating the run of a pipe when the pipe was excited vertically at the surface with an inertial shaker. Frequency response measurements relating vibrational velocity on the ground to the input excitation were acquired. Contour plots of spatially unwrapped phase revealed the location of the pipe to within 0.1 m-0.2 m. Magnitude contour plots revealed the excitation point and also the location of the pipe end. By examining the unwrapped phase gradients along a line above the pipe, it was possible to identify the wave type within the pipe responsible for the ground surface vibration. Furthermore, changes in the ground surface phase speed computed using this method enabled the location of the end of the pipe to be confirmed.

For the ground excitation, as for the pipe-excitation method, time-extended signals are used to generate an illuminating wave. A stacking method is then employed, which involves the measurement of velocities on the surface of the ground. Cross-correlation functions between the measured ground velocities and the excitation signal are then calculated and summed to generate a cross-sectional image of the ground. The wide cross-correlation peaks caused by high-ground attenuation are partially compensated for by using a generalised cross-correlation function called the smoothed coherence transform [12].

2.1.3. Low-Frequency Electromagnetic Fields. The LFEM sensor, implemented using frequency domain processing, has been developed from first principles for the project. It has been included within the multisensor device since it has the potential to complement GPR by locating utilities that GPR would have difficulty in detecting. Examples include small diameter plastic pipes and fibre optic cables, pipes that lie in the blind zone of GPR, and large deep buried infrastructure, such as deep sewers, that lie beyond the range of traditional methods. The LFEM sensor works by inducing a small current through the ground using capacitive coupling, in response to which a quasistatic electric field is

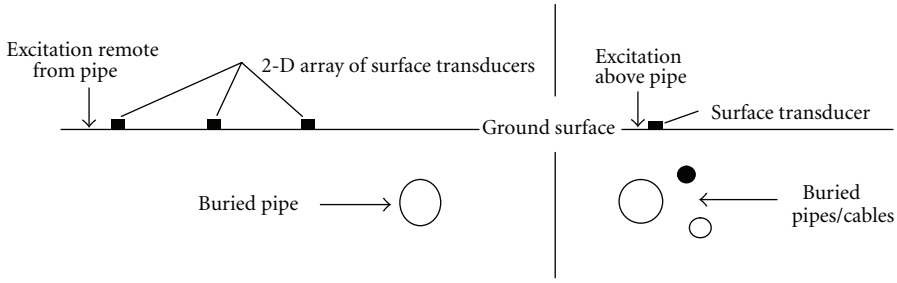

FIGURE 5: Illustration of pipe detection with vibro-acoustic sensing technology via ground excitation (a) offset from the utility and (b) directly above the utility. Note that the excitation can be normal or parallel to the ground surface, or a combination of both (first published in [7]).

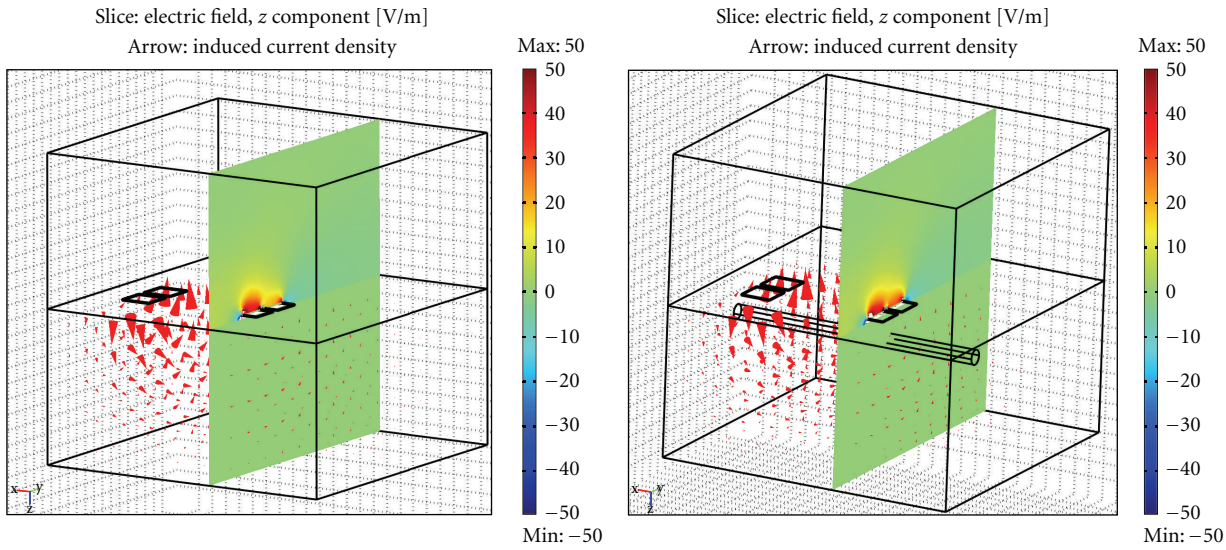

FIGURE 6: Finite element simulation of the near-surface electric field without pipes (a) and with pipe (b) (images previously published in Royal et al. [5]).

generated. Any materials that present a contrast in electrical properties to the soil will disturb the induced current flow [13–18]. By using precisely controlled digital-to-analogue signal converter generating voltages at two transmitting capacitive plates, anomalies in the electric field near the surface resulting from the disturbance of current density in the ground can be detected (Figure 6) by using an ultrahigh impedance amplifier connected to receiving capacitive plates. The synchronisation of the anomalies detected during the survey with the positional data for the multisensor device during the survey allows for the prediction of the position of the buried utilities. The depth can then be evaluated using inversion methods analogous to techniques in resistivity imaging [14].

The frequency selection strategy for this sensing technology is based upon avoiding strong ambient EM fields (e.g., 50 Hz and its harmonics) as well as interfering components from other sensors. This can be accomplished by first measuring the ambient field without active transmission across the valid frequency range of 1 Hz to 25000 Hz and adaptively selecting the frequency component with the least energies. The transmission frequency must also be above the constraint imposed by the cut-off frequency associated with the physical dimension of the transmission plates. The transmission frequency was 1.735 kHz in this trial.

2.1.4. Passive Magnetic Fields. The flow of current within a buried AC power cable creates an associated oscillating magnetic field, which the PMF sensor can detect. Current flow within the power cable can also induce currents within neighbouring utility pipelines or ducts made from conducting materials, such as cast iron, and the PMF has the potential to detect these utilities also. Programs are being developed to use the detected signals to locate and identify various types of buried power cable or other conducting services. The PMF sensor comprises an array of passive search coils arranged in a 3D configuration to detect the magnetic field.

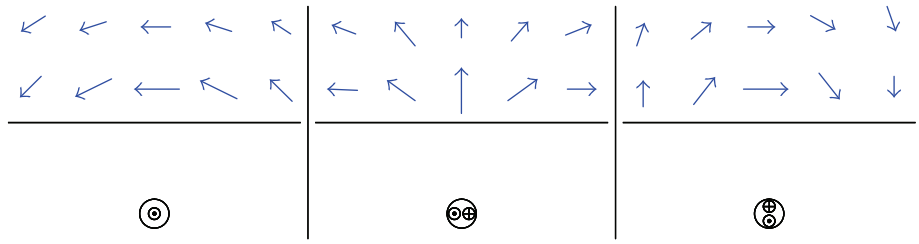

Figure 7: Illustration of the concept underpinning the detection of operational power cables using multiple passive search coils. The arrows show the flux density distribution due to three different current distributions in the power cable. The field plots shown are for a hypothetical untwisted cable, as the field of a more realistic twisted multi-core cable is difficult to represent in 2D.

Initially seven, though shortly to be increased to 27, passive search coils mean that the magnetic field can be measured at many positions simultaneously. Using simultaneous measurements of the flux in the various coils of the PMF sensor allows for the estimation of the cable position (Figure 7) by comparing the magnetic field recorded to theoretical responses for various types and configurations of power cables (three phase cables, single phase cables, cables with balanced or unbalanced loads, straight or twisted cables, etc.).

3. Outcomes from Preliminary Testing

To meet the aim of this MTU project, that is, to demonstrate the ability to detect *all* utilities buried below the carriageway, a comprehensive programme of proving trials is planned to assess the capability of the prototype device. However, as the sensing technologies and their deployment strategies are being developed it is important that initial phases of testing on sites containing simple utility layouts, with known positions, are carried out. The first phase of testing occurred at a site located near Blithfield reservoir in Staffordshire (Figure 8). The test site was specifically created to permit the investigation of leakage detection in water distribution pipes using acoustic technologies, and as such comprises a buried water pipe (over 100 m long) with several access points spaced along the pipe allowing for the simulation of leaks via a shaker or standpipe. The site also contains a buried electricity cable, thus allowing for the testing of all sensor types being developed for the project.

Initial site testing took place on three occasions in July, August, and November 2010: the PMF, dual-frequency pulsed GPR, and LFEM were deployed independently during the first visit; the GPR and LFEM were combined on the second occasion and the vibro-acoustics surveyed on the final occasion. Initially the section of the site selected for testing was surveyed with the commercial GPR using a coarse 1 m grid, and both utilities were readily detected. Having located the utilities' plan location and estimated the depths with the GPR, the prototype sensing technologies were deployed. The LFEM and vibro-acoustic sensing technologies were used to locate the water pipe and the PMF sensor the cable. The vibro-acoustic testing involved both pipe and ground excitation methods (Figure 9), with measurements of vibrational velocity on the ground (in three orthogonal directions, using 3-axis geophones). The geophones were deployed using a both a grid pattern (for the pipe excitation method) and single lines traversing the pipe (for the ground excitation method). The grid used was 16 m long and extended 1.5 m on each side of the pipe, taking measurements every 0.5 m and using the centreline of the pipe as the baseline for the survey; the single lines each employed 7 geophones spaced at 1.0 m intervals. The LFEM survey was undertaken using GPS to provided positional information instead of following a grid pattern within the area of interest, taking the fence line as the baseline for the survey. The PMF sensor took readings at 16 points along a 4.5 m survey line that crosses the cable, again taking the fence line as the baseline for the survey.

3.1. Vibro-Acoustics. Two pipe excitation methods were used at the test site: an inertial shaker was attached at an access point (as used in previous work by the vibro-acoustics team), and "leak" noise was generated by opening a standpipe connected at the same access point (Figure 9). It was anticipated that, using either method, the wave predominantly excited in the pipe would be the axisymmetric, fluid-dominated wave [19], this being the preferred wave type. For both pipe excitation cases, frequency response measurements relating the vibrational velocity on the ground to the input excitation were acquired. In the case of the shaker excitation (a 2-minute swept sine input from 10 Hz to 400 Hz) the voltage input to the shaker was used as a reference, while for the "leak" noise excitation an accelerometer was located adjacent to the standpipe (visible in Figure 9(a)), the measured acceleration being used as the reference. It was found that the simulated leak excited the preferred wave in the pipe more effectively than the inertial shaker, with the straight-line frequency-unwrapped phase behaviour evident at frequencies between 30 Hz and 200 Hz at all grid locations in this case. For the shaker excitation, the upper cut-off for some grid locations was 100 Hz with the lower bound increasing in some cases to around 50 Hz. Data from both excitation types were found to be useful in inferring the pipe location, with the data from the "leak" excitation being superior. Contour plots of the spatially unwrapped phase for both the vertical velocity and horizontal (aligned parallel with the pipe) velocity measurements in the frequency range 40 Hz–80 Hz revealed the location of the pipe for this excitation type. Two sample frequencies (42 Hz and 72 Hz) are shown in Figure 10. At 42 Hz, the vertical geophone measurements

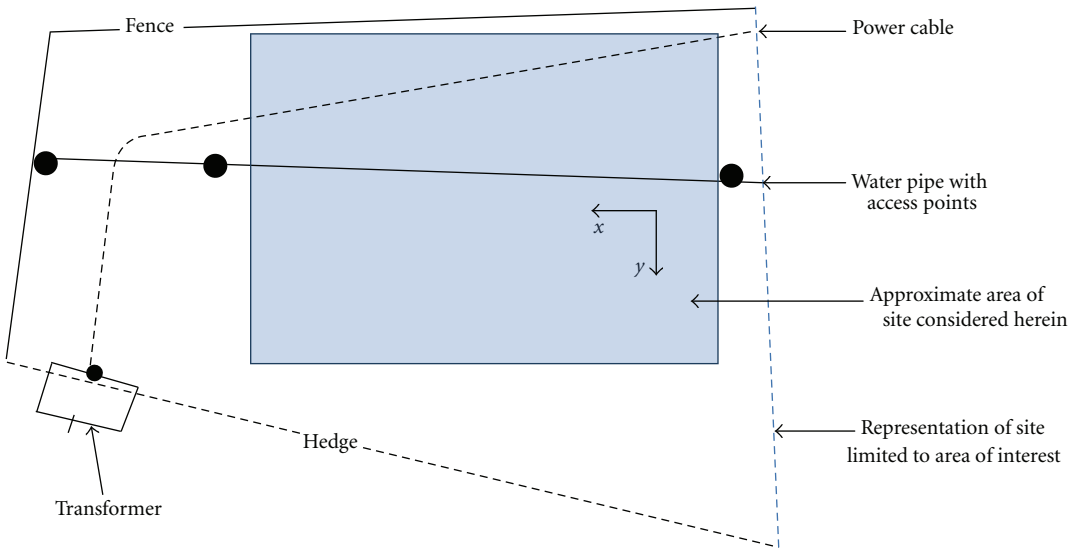

Figure 8: Layout of the Blithfield test site.

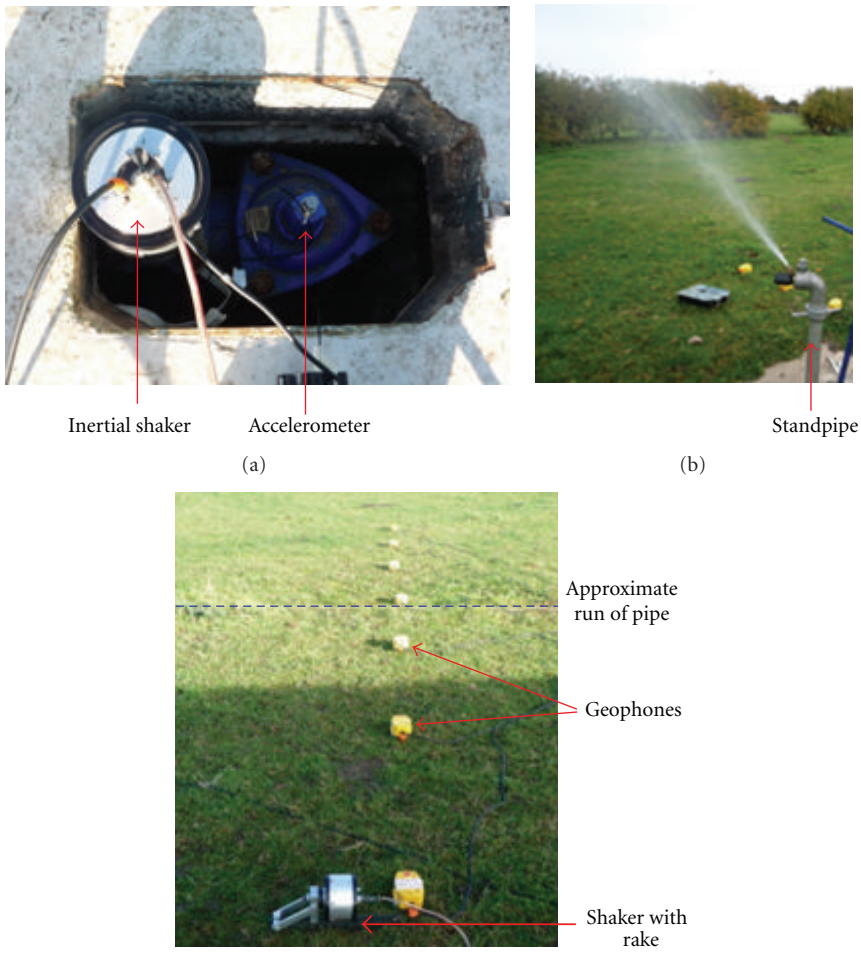

Figure 9: Excitation of (a) the pipe via inertial shaker, (b) the pipe via standpipe, and (c) excitation of the ground using an inertial shaker with rake attachment.

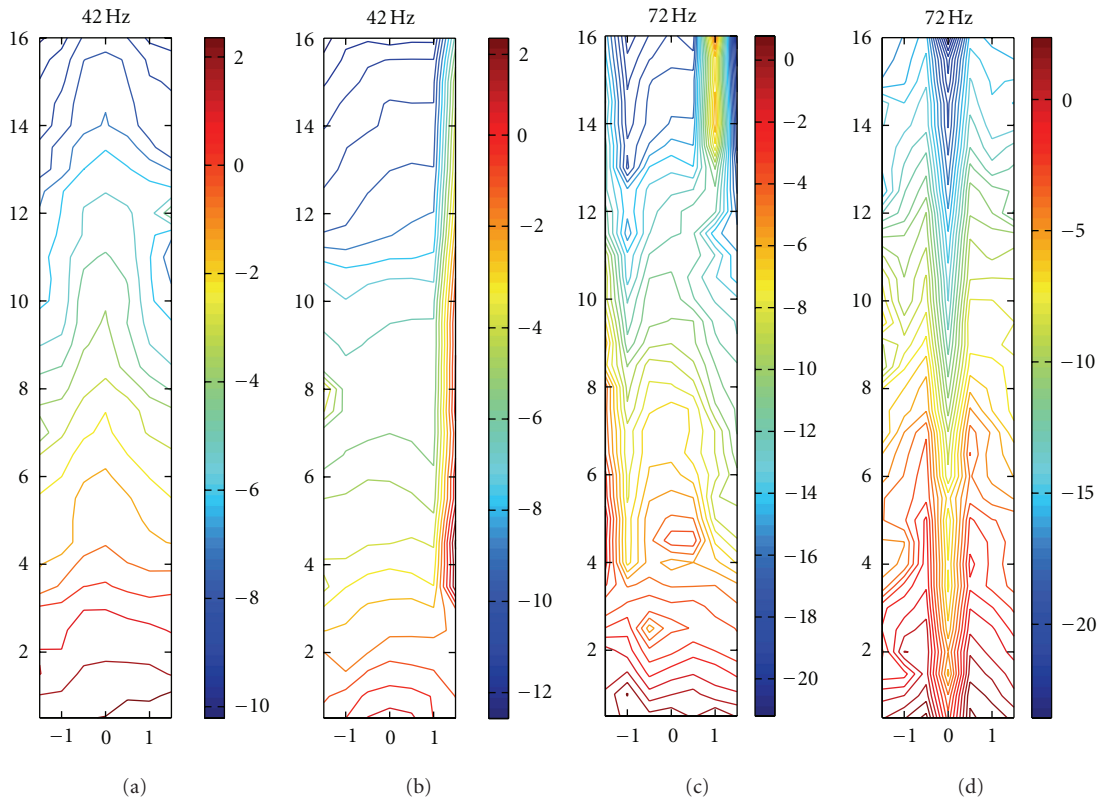

Figure 10: Contour plots of spatially unwrapped phase for simulated leak noise in each plot, the x- and y-axes correspond to the axes shown in Figure 8 rotated by 90 degrees; the unwrapped phase is shown in radians; the pipe runs up the centre line in each plot (a) vertical measurements: 42 Hz; (b) horizontal measurements: 42 Hz; (c) vertical measurements: 72 Hz; (d) horizontal measurements: 72 Hz.

clearly show the run of the pipe; at 72 Hz, the horizontal measurements show this more convincingly.

The ground excitation method employed at the test site was similar to that used by [20, 21], using a configuration similar to that shown in Figure 5(b); the pipe was thought to be buried too deeply for the point measurement method (Figure 5(a)) to be employed successfully. The ground was excited horizontally in order to preferentially excite horizontally polarized shear waves (these have been found to give more reliable results than using compressional waves). Directionality (a desirable feature) was achieved via extended contact with the ground, using a rake attached to the inertial shaker. Again a 2-minute swept sine input from 10 Hz to 400 Hz was employed. The surface vibration velocity was measured using a line of 7 geophones perpendicular to the run of the pipe, with a spacing of 1 m. The rake was placed in the ground so that the motion of the shaker was parallel with the pipe, thus producing shear waves travelling across it (the arrangement is shown in Figure 9(c)). The shaker and rake assembly was positioned at each geophone location in turn, thus enabling the stacking to be performed over 49 (7×7) source-receiver position combinations. Stacking requires that the shear wave velocity through the ground is known. This is calculated from the time delay associated with peaks in the correlation function at different source-receiver positions. Different pairs of positions will give slightly different results so there is always some uncertainty in the final estimated wave speed (which, of course, may vary slightly from location to location). With this in mind, a range of speeds was used in performing the stacking and obtaining the final cross-sectional image. In this case, wave speeds of 65 m/s, 70 m/s, 75 m/s, 80 m/s, 85 m/s, and 90 m/s were used. Figure 11 shows the cross-sectional images obtained along with the geophone positions on the surface and the estimated location of the pipe (black circle—obtained from burial records). A dark red area can be seen in all the plots in the vicinity of the black circle (Figure 11), indicating the presence of a target. Examining the figures as a whole it can be seen that the perceived depth of the target increases with increases in the estimated wave speed, varying from approximately 0.8 m at 65 m/s to 1.7 m at 90 m/s. Laterally, the perceived position varies by around 0.3 m, slightly to the right of the expected location. The precise pipe burial location relative to the geophone positions was not confirmed by other means at the time of testing.

The results of the testing using vibro-acoustics corroborated the previous evidence of the ability to detect a buried utility using pipe excitation and the results from the initial ground excitation experimentation were encouraging. The vibration results from the ground excitation contain uncertainties and more work is needed to refine wave speed estimation, and so forth, as well as developing possible refinements to how the data are captured (e.g., geophone spacing) and processed. Excitation of the ground removes the

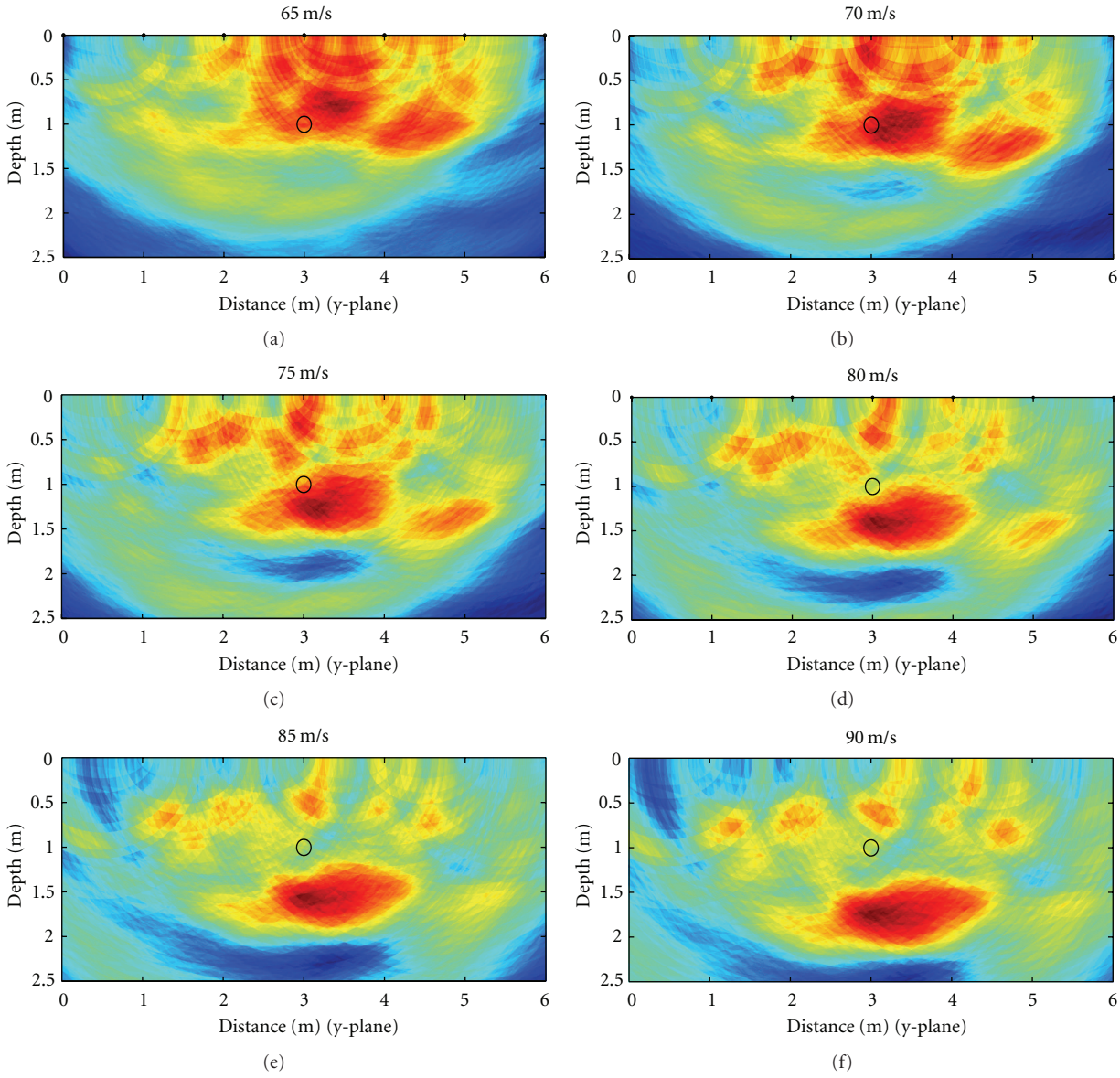

Figure 11: Cross-sectional stacking images using 6 different estimated wave speeds.

requirement for access to the utility, thereby greatly improving the potential flexibility of vibro-acoustics to detect utilities. Combining data from the different technologies could resolve the uncertainty attributed to this approach.

3.2. Passive Magnetic Fields. A seven-search-coil assembly was used on the test site (Figure 12). It was connected to an eight-channel data acquisition system and was manually moved along the heading chosen such that it crossed the power cable. The frame was aligned to the local coordinate system selected for the survey (the fence line in this case), and the new position measured and entered into the data acquisition program. These coordinates were added to the relative positions of the coils on the frame, which are loaded from a file. In the final prototype multisensor deice it is envisaged that the positional information required to analyse the PMF data will be provided by common positional sensing technologies (which will measure changes in inclination and azimuth with time) mounted on the platform.

Figure 13 illustrates the outcomes of the data analysis for a section of the survey undertaken with the PMF sensor. The image represents an error contour map, with the contours representing the proportion of the field that could not be explained by the magnetic field generated by any straight cable at the plotted position. This minimum error is generated for a cable position of $y = 3.5$ m, an apparent depth of 0.37 m, a heading of -12.4°, a twist rate of -4.65 rad/m; the returned error at this location is 3%. This positional information contradicts the utility records, which suggest that the cable position at this location is given by $y = 2.5$ m, with a depth between 0.4 m and 0.6 m and a heading of -13° (Figure 13). Based on the estimated currents for the best-fit parameter values, a 3-phase factor has been calculated. The value of this parameter can vary from zero

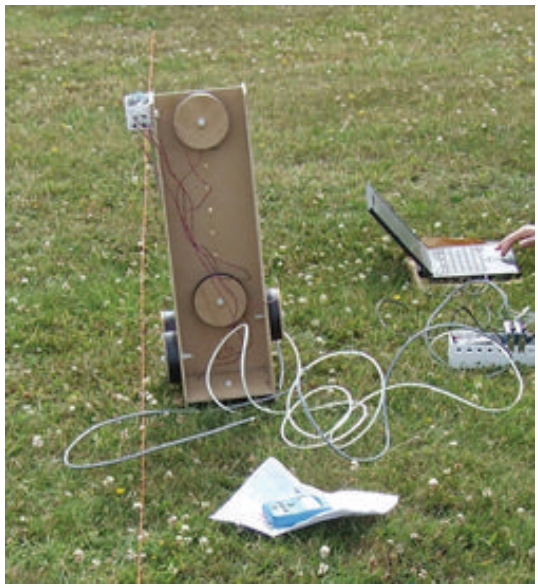

Figure 12: The prototype PMF sensing technology.

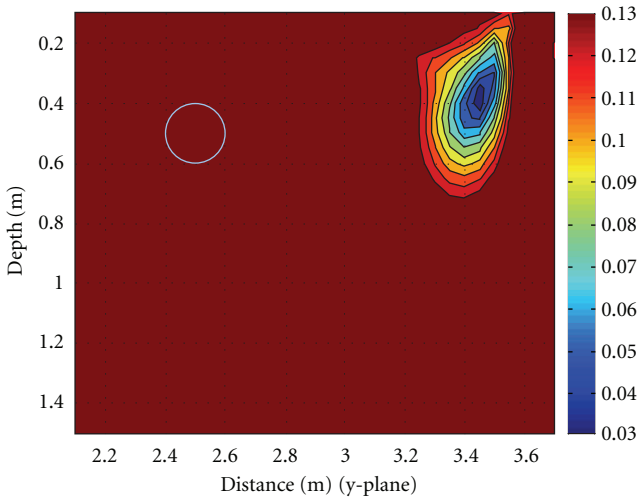

Figure 13: Error contour map generated from the recorded magnetic field, with the cable location most likely to occur where the errors are the least. The position of the cable according to the records is shown as a circle.

for a 2-core single-phase cable to 100% for a 3-core 3-phase cable with a balanced load. The calculated value of 62.1% could indicate a 3-phase cable with a very unbalanced load, a single-phase cable with substantial neutral-earth loop current, or a single phase cable that is not straight and has a net current. With reference to the transformer, it is visibly evident that there is only a single-phase supply, and hence it must be a single-phase cable. To distinguish between the two remaining interpretations would require measurements to be taken over a wider range of headings that cross the cable position, whereas all the measurements used to produce these results were taken with the support frame centred along one heading.

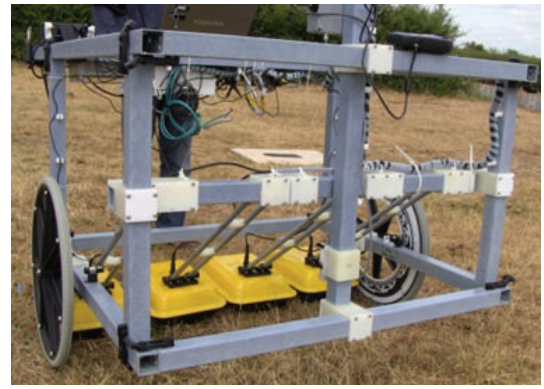

Figure 14: Prototype sensor platform deployed at the Blithfield test site (illustrating the LFEM sensor).

The outcomes of the PMF testing are encouraging and demonstrate the ability of the system to locate a power cable in an uncluttered environment. Further development is required for this detection technique to be effective in more cluttered urban environments. Ultimately, it should be possible to locate and identify different types of buried power cables and to locate other metal utilities that carry earth currents or currents induced by the magnetic field generated by operating power cables.

3.3. Ground Penetrating Radar and Low-Frequency Electromagnetic Fields. GPR and LFEM surveys were undertaken sequentially during the first visit to the site and were later followed by a combined GPR-LFEM survey with the sensing technologies mounted on a prototype platform (Figure 14). In each of these tests the sensing technologies were deployed using a dynamic test protocol, in which the GPR and the LFEM sensors are pushed across the site. The GPR was successful in detecting the two utilities of interest on the site during the first site visit in July, when the weather had been hot and dry for a reasonable period of time. As a result of the ground being relatively dry, the hyperbolae visible on the real-time display were very distinct (Figure 15(a)). Expressing the GPR as a plan view allows for the location of the pipe within the surveyed area to be determined (Figure 15(b)). Plotting the GPR data in such a format also allows for the comparison in performance of the LFEM sensor (Figure 15(c)). The LFEM sensor has identified anomalies within the site, as expected, and encouragement is taken from the accumulation of anomalies detected along the length of the pipe (highlighted by a red dotted ellipse on Figures 15(b) and 15(c)). The anomalies detected near the known location of the pipe (Figure 15(c)) exhibit variation in position when plotted in a plan view. This is partly due to the speed of survey (>0.5 m/s) which limited the signal-to-noise ratio of the collected data. This can be addressed with increased transmission voltage in order to maximise current flow in the ground. It also transpires that these variations can be attributed, in part, to the positioning system employed during the test. Two GPS systems were used with the LFEM sensing technology: a kinematic GPS for positioning and a secondary conventional GPS system for time synchronisation

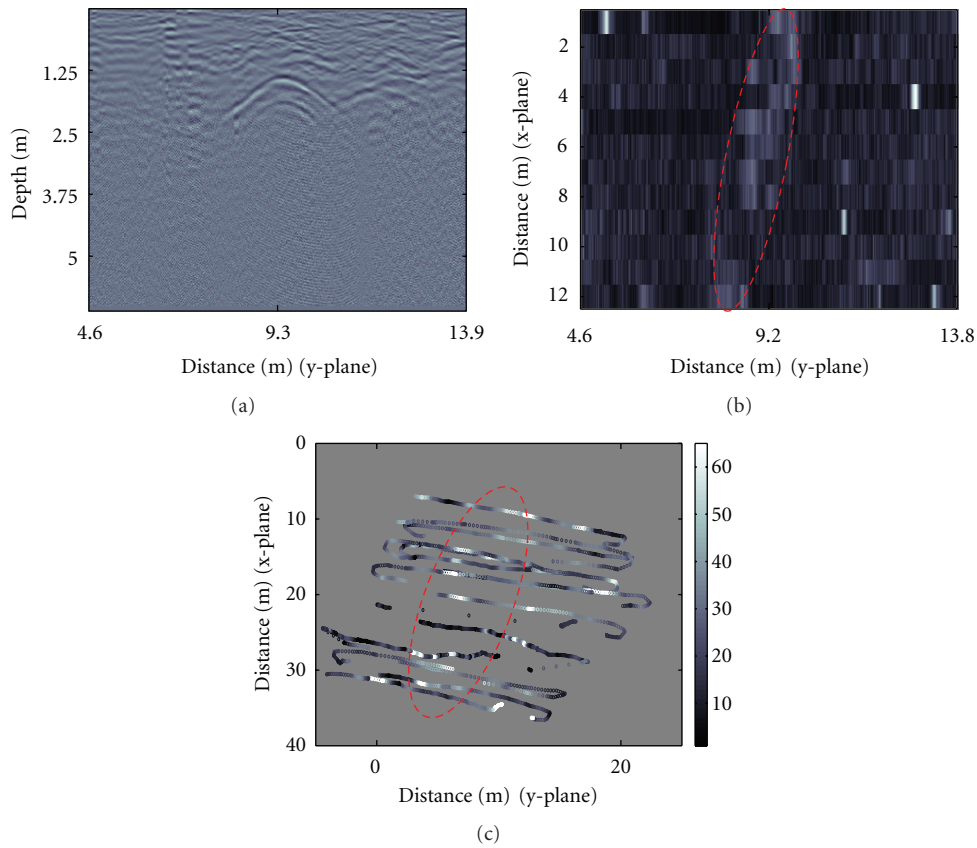

Figure 15: GPR results (250 MHz) from initial survey: (a) hyperbola returned when directly over the pipe, (b) plan view of the GPR survey (averaged at depth slices where the hyperbolae are prominent), and (c) the LFEM survey (overlaid onto the GPS positions within the predefined area), where a brighter region represents higher anomalous measurement.

(which was not suitable for precise positioning). Subsequent data analysis illustrated that the data from the kinematic GPS was corrupt, resulting in reliance on the conventional GPS system for positioning. Significant positional errors (of the order of one to two metres) were suspected as the brighter pixels indicating anomalies do not align linearly in the region where the target pipe is known to be buried. The outcome of this test thus highlighted the need to capture kinematic GPS data with short epochs to identify the position of the platform when on site. This amendment notwithstanding, the initial trial results were considered to be promising.

3.4. Potential Conflicts When Combining the Sensing Technologies. The four sensing technologies have not yet been mounted on a single platform, although the commercial GPR and prototype LFEM sensing technologies were successfully combined. However, the research team has identified a number of potential conflicts that are being addressed as the design of the prototype multisensor platform is advanced.

The combination of the GPR and LFEM sensors created no apparent conflicts when analysing the results. This was attributed to a difference in survey speeds, with GPR requiring milliseconds and the LFEM being developed to operate, at least initially, in the decisecond range. This has led to the proposal for a sequential protocol for sensor deployment, with the GPR sensor acquiring and storing data whilst the other sensing technologies are "passive"; analysis of the GPR data can then take place whilst the other sensing technologies are triggered (Figure 16). The difference between the rates at which GPR and the other sensing technologies acquire data makes this a feasible strategy and in large part addresses the concerns arising from co-location of the GPR sensor. However, the survey speeds of the LFEM, PMF, and vibro-acoustic sensing technologies are such that it is believed that these surveys must be undertaken concurrently to ensure the advance rate of the multisensor platform is not compromised.

Potential conflicts between the LFEM and PMF sensing technologies have been identified:

(i) the magnetic fields associated with the current injection of the LFEM could be detected by the PMF,

(ii) currents could be injected into the search coils via stray capacitance,

(iii) the plates used in the LFEM could distort the magnetic field associated with the buried cables.

In order to minimise these potential conflicts, the frequency used by the LFEM has been raised to 16.67 kHz, thus minimising interference with the multiples of 50 Hz that are produced by AC power transmission. Moreover, the current injected by the LFEM technology is to be low

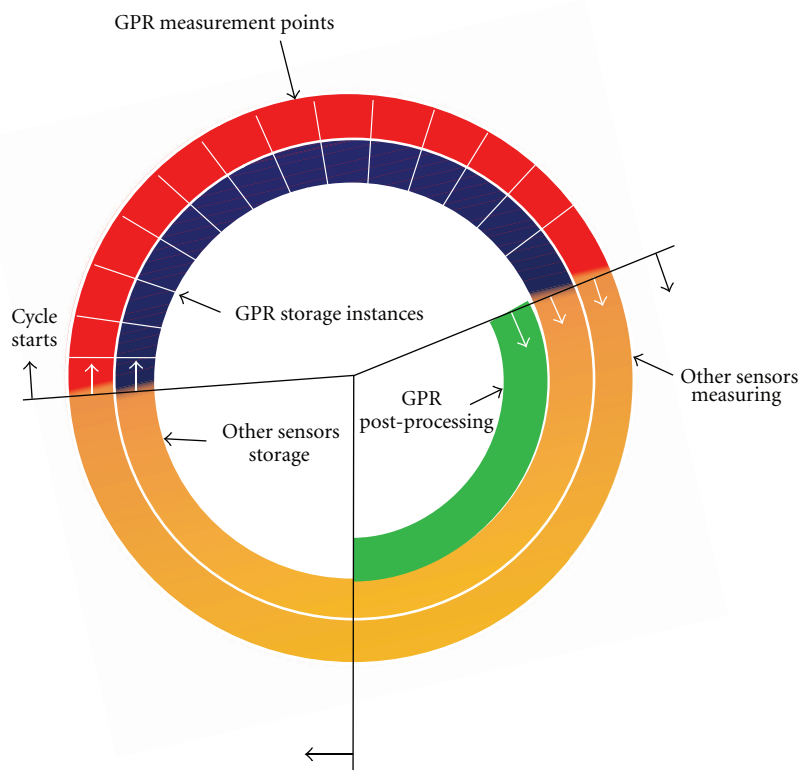

Figure 16: Schematic representation of data acquisition, storage, and processing.

(in the milliamp range), and the capacitance plates used in the LFEM are shielded with an aluminium cover. However, these precautions are not without limitations: whilst the shielding will greatly reduce the cross-coupling, it increases the distortion of the magnetic field caused by power-frequency eddy currents in the LFEM sensors, thereby reducing the benefit of using more coils. The current injected by the LFEM system will still induce voltages within the search coils, but the high frequency of the injected current makes it relatively easy to filter away the unwanted signal. For the chosen frequency and amplitude of the injected current, a minimum separation of 200 mm between the LFEM current leads and the PMF coils should ensure that these voltages are not significantly larger than those that the search coils are looking for; filtering can then be used to give adequate signal-to-noise ratios. Distortion of the field by the presence of the LFEM sensors is a bigger problem, as neither filtering nor time sharing will help. Simple modelling suggests that if the PMF coils are maintained at least 640 mm away from the LFEM plates, the distortion will be limited to about 1%. Until these conflicts can be quantified, the sensing technologies mounted on the multisensor platform are to be separated to minimise the potential effects of these conflicts. It is appreciated that a spacing of 640 mm between LFEM and PMF sensing technologies will make the platform relatively large, which would be undesirable for a commercial platform. However, as the platform is being developed as a prototype "proof of concept" device, its size is relatively unimportant at this stage. If, when the conflicts have been quantified, the required separation is considered too large, alternative measures would have to be used to overcome the problem. Potential conflicts between the vibro-acoustics and other sensing technologies are currently being considered.

4. Intelligent Tuning of Sensing Technologies to the Ground

The MTU philosophy contends that in order to optimise the efficiency of the multisensor platform, the ground conditions in which the survey is to be undertaken should be known, as far as possible, and the implications of the ground conditions on the performance of the sensing technologies understood, prior to the deployment of the device on site. Such knowledge and understanding would allow the surveyor to identify the conditions where certain sensing technologies will perform significantly better or worse than the others, and thus potentially increase the probability for detection of the utilities on the site. For example, electrically conductive ground conditions cause significant attenuation losses of electromagnetic signals, resulting in shallow penetration depths for GPR. Knowing that such ground conditions are likely to be met on site might encourage a change in deployment of GPR from the traditional surface mounted "look-down" surveying to the adoption of the "look-out" or "look-through" modes of surveying with the use of the in-pipe GPR (Figure 2). Conversely, an alternative sensing technology, such as vibro-acoustics, might be selected as the primary sensor, with GPR being chosen to act as a back-up device in locations where it is deemed appropriate.

Therefore, one of the aims of the project is to develop a system that can be used to predict how the ground conditions will impact on the performance of the sensing technologies before deployment occurs.

The basis of the predictive tool being researched thus relies upon information on the ground conditions at any specific location, which in itself is not straightforward due to the type of information commonly available. The *geotechnical* properties of shallow ground conditions can be relatively well characterised within the UK. Databases such as the National Geotechnical Properties Database (NGPD maintained by the British Geological Survey, BGS [22] and the soil properties map (maintained by the National Soil Resources Institute and geared towards agriculture science), along with data published in the literature, comprise a large collection of soil properties nationwide. However, whilst geographical variation in soil properties within the databases is apparent, there is little readily available information on the seasonal variation in soil moisture content, a factor that directly affects soil electromagnetic properties [23]. In addition, the *geophysical* properties of soil are often poorly characterised, with limited information within the public domain. The geotechnical (and limited geophysical) property data available within databases and the literature are predominately based upon drilling records and/or site/laboratory investigations. Whilst the information will act as an informative guide for the nature of the likely soil formation(s) to be encountered, the data only strictly relate to the specific site originally investigated. Moreover, the heterogeneous nature of soil, the natural variations in properties with depth, and the many anthropogenic alterations to the ground in urban areas suggest considerable potential variation and thus the information is indicative only.

While a simple prediction model for soil behaviour on a site would be desirable, it is believed that such an approach alone would struggle to predict the impact of the ground conditions on the performance of the sensing technologies. Instead it is proposed that a system with the ability to interpret a wide range of available information be adopted, drawing on a wide knowledge base that utilises *any* available input parameters in order to predict the electromagnetic properties of the ground. In turn, these need to be robustly related to the performance of the sensing technologies. This is the key motivation for implementing a knowledge-based system (KBS) approach for this work. The design of the KBS is illustrated in (Figure 17). The main output from the KBS is the prediction of the geophysical properties associated with individual sensing technologies. This data can be used to guide the survey by providing prior estimates of the suitability of individual sensing technologies to a survey site. The fine-tuning of the sensing technologies can then be carried out locally using estimates of ground properties obtained from the KBS together with those inferred from individual sensing technologies and (where possible) the results of in situ tests that directly measure geophysical ground properties.

There are three key inputs to the KBS to be used alongside expert, *a priori* knowledge: the link between available geotechnical properties of the soil and its electromagnetic properties, the seasonal variation of the soil moisture content with depth, and the opportunistic approximation of soil properties based upon individual sensing technologies and in-situ tests. As stated previously, the availability of geophysical properties of a soil are typically limited, therefore additional research is being undertaken to develop test apparatus to readily measure the geophysical properties of various soils and further the understanding of the correlation between geotechnical and geophysical properties of soil technologies [24–28]. Research is also being undertaken to broaden the understanding of the relationships between changing seasons and recent weather, variations in soil water content profiles with depth [23], and the resulting geophysical properties for various soil types.

4.1. Linking Soil Geotechnical Properties to Its Electromagnetic Properties. The literature on soil electromagnetic properties presents a number of modelling and prediction methodologies. A review of these can be found in [29]. In the KBS, the model being adopted is the semiempirical mixing model that relies upon soil composition and moisture content, based upon the work of Peplinski et al. [30], Mironov et al. [31], and Dobson et al. [32]. The choice of this model is desirable given the availability of soil composition data from the NGPD, while soil classification tests are routinely performed on soil samples extracted in association with construction work being carried out in urban areas. The KBS should, and can, allow for the incorporation of additional modelling methodologies as well as the refinement of integrated models. Therefore, the choice of this semiempirical model presents a starting point for the implementation of the KBS and does not define its limitation.

Testing was undertaken at the Blithfield site using time domain reflectometry (TDR) and a coaxial sensor (developed for the project), in conjunction with the semiempirical model. A soil composition of 30% sand, 65% silt, and 5% clay was used in the model, based upon the particle size grading as specified in ISO 14688 for the identification and classification of soil. The bulk density was estimated to be 1.2 Mg/m^3, while a volumetric water content of 8.2% was calculated by applying the model by Topp et al. [33] to the in-situ measurement carried out with the TDR. The complex permittivity predicted is shown in Figure 18, with the result demonstrating good agreement with the values obtained from the direct measurement of soil electromagnetic properties using coaxial probes, as described below.

The seasonal variation of soil moisture content can also be modelled and predicted. The work by Saxton et al. [34] and Saxton and Rawls [35] is being used as the basis for empirical modelling of soil water characteristics based upon soil composition. Assuming a noncovered surface, this model enables the prediction of water infiltration rate with respect to depth, and subsequently the variation of soil moisture content caused by weather events. A total of four long-term monitoring stations that measure the apparent permittivity and conductivity of the soil are being installed on sites with different soil composition [23]. Data collected from these monitoring stations are expected to provide experimental

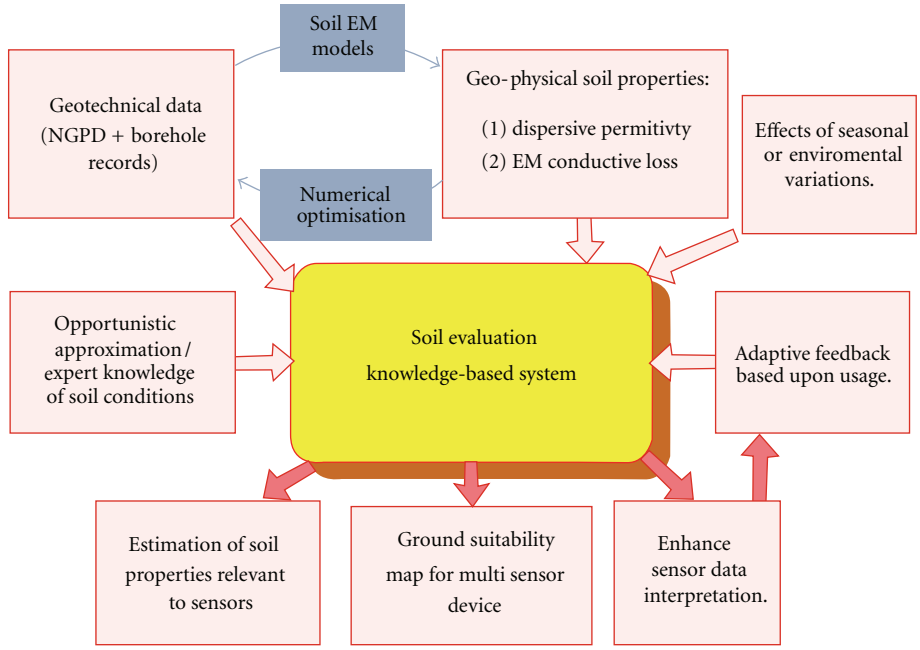

Figure 17: Illustration of the concept behind the soil evaluation knowledge-based system software.

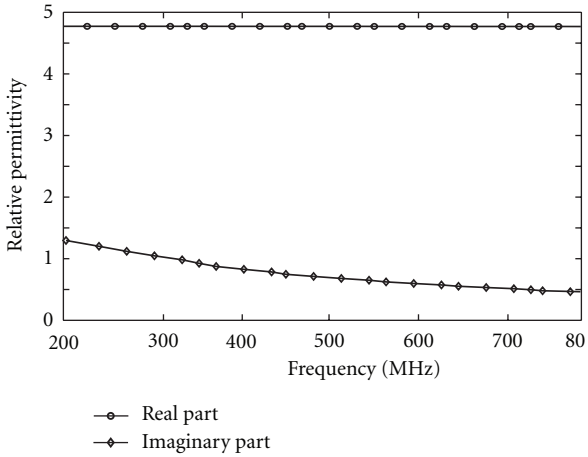

Figure 18: KBS modelled complex permittivity of the soil at the Blithfield test site at depth of 280 mm.

comparisons and validation of the model applied herein. This model was not necessary for the Blithfield test site as the moisture content was measured in-situ with a TDR. A simple test site has also been constructed at the University of Birmingham using TDR probes to measure changes with water content in a soil with depth and season.

While analytical models are useful in providing an estimation of soil conditions, they remain a generalised solution for a very wide set of unique input parameters. Therefore, as part of the KBS strategy (Figure 17), opportunistic approximation and input based upon expert knowledge and experience should be taken into account. As the LFEM sensor produces a measure of apparent resistivity, it may be possible to derive an estimate of electrical conductivity of the soil while a survey is being carried out, or very soon after. A protocol is also being designed to extract information from the user based upon experience or visual observations, such as the conditions of road surface or pavement, whereby a positive visual observation of surface degradation may imply the possibility of water infiltration. As it was possible to dig on the test site, these methodologies were less significant because moisture content was measured with the TDR and deemed to be more reliable in this specific scenario.

4.2. Measurement of Soil Electromagnetic Properties. Analysis is being conducted, both *in situ* and in the laboratory, on the links between soil characteristics and its impact on the sensing technologies' performance, not only to provide an experimental means to validate and quantify the predictions of the KBS, but also to contribute to the body of knowledge that underpins the direct study of soil electromagnetic properties. This involves the design of sensing devices and techniques specifically for the direct measurement of soil electromagnetic properties *in situ*.

The dependence of utility location technologies such as GPR on the electromagnetic properties of the soil can be explained by (1) [36], where L represents the attenuation losses due to the soil, R is the distance from the GPR antennas to the target, f the frequency in Hz, c the speed of light in a vacuum, $\tan\delta$ the loss tangent of material, ε_r the relative permittivity of material, ε_0 the absolute permittivity of free space (8.854×10^{-12} farad/m), μ_r the relative permeability of material (for the underground applications considered herein the permeability is usually 1), and μ_0 the absolute permeability of free space ($4\pi \times 10^{-7}$ Henry/m). The research undertaken in this area for the project has concentrated on obtaining the relative permittivity ε_r of various soils. Several semiempirical models based on soil composition have been developed to predict the permittivity of soils [29, 30, 36]. Due

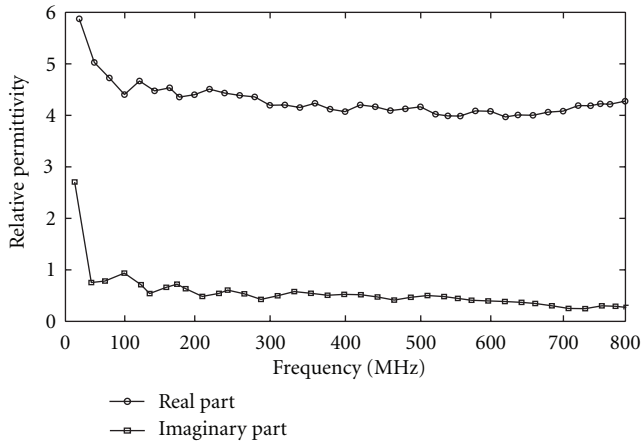

Figure 19: The measured permittivity at 280 mm depth at the Blithfield test site, using the open-ended coaxial probe (July 2010).

to the nature of the semiempirical approach, the accuracy of the models is highly dependent upon and restricted by the soil types used to develop the models, which means other soils with different compositions are predicted with less accuracy

$$L = 20\log_{10}\left(2 \times R \times \frac{2\pi f}{c}\sqrt{\frac{\mu_0\mu_r\varepsilon_0\varepsilon_r}{2}\left(\sqrt{1+\tan^2\delta}-1\right)}\right). \quad (1)$$

The TDR technique [37] is well developed and widely used in measuring the apparent permittivity of soils. It is noted that this approach gives a single permittivity value over a range of frequencies, which means the dispersive characteristics of lossy soils along the frequencies cannot be explained. More recent frequency domain techniques such as resonant cells and open-ended coaxial probes can measure this over a defined frequency range [38]. In particular, the resonant cell was used to measure the properties of fine-grained soils [26], while coaxial probes are used to carry out localized soil measurements. A large open-ended coaxial probe was built to measure various types of soils, including Leighton Buzzard sand, Oxford clay, and soil samples from the trial site. The analytical approach is used to calibrate the probe, and the results show good agreement between the coaxial probe and TDR, while the dispersive characteristics of soils are explained by the coaxial probe. As one example, the complex permittivity of soils at a depth of 280 mm at the Blithfield test site is shown in Figure 19. The TDR measured apparent permittivity was 4.74 at the same depth. The coaxial probe was also tested at another field site on the campus at University of Birmingham in July 2010 with similarly encouraging results, the comparison between the coaxial probe and TDR being shown in Table 1.

The design of flangeless open-ended coaxial probes with curved surfaces is also being investigated. The degree of the curvature (concave and convex) of the surface is selected to be about 16°, in which case the probes with these curved surfaces can still be modelled using the quasistatic approach that has been widely used for the probes with flat surfaces.

Table 1: Comparison between the measured real part of the permittivity and apparent permittivity by the coaxial probe and TDR at a test site at the University of Birmingham.

	Coaxial probe	TDR
At 10 cm depth	2-3	1.8
At 110 cm depth	5–8	6.8

The probes with curved surfaces are of potential value in applications where such probes must be assembled onto drilling devices widely used in fieldwork.

5. Fusion of Sensor Data with Buried Asset Records

5.1. Buried Utility Pipeline Mapping Based on Street Surveying and GPR. Utility maps are often produced from a combination of street surveys and geophysical scans. The surveyors will routinely investigate the on-site street furniture, such as manholes, as this is useful information regarding the utilities on site. Identification of street furniture positions provide information that can fit the utilities to a known surface location (assuming that the manholes are still in use and are connected to services) and provides information on the possible direction of these pipes as a starting point for a survey. However, this information is insufficient when producing utility pipeline maps as the underground environment is typically crowded and utilities do not necessarily transit directly between access points; bends, changes in direction, changes in depth, and tee-junctions could all conceivably occur between the known locations (assuming that the utility in question indeed runs between the these access points). Thus GPR and other geophysical surveying techniques will be usually employed to verify these hypotheses.

By combining the street survey and GPR data a utility map can be generated, employing techniques akin to those used in robotics [39]; in robotics new sensor measurements are associated with existing map landmarks before fusing data into the map. The problem can be viewed as a search problem in the space of observation-feature correspondences [40]. When mapping utilities, the data association is the connection of the observed manhole and GPR detection, that is, determining the pipes among the observed information from manholes and GPR data analysis. The map connecting problem is critical as a single incorrect association can induce divergence into the map estimate, often causing catastrophic failure of the algorithm. When developing the utility mapping algorithm for the project, two approaches were employed: Nearest Neighbour standard filter and Joint Compatibility Branch and Bound (JCBB) methods.

The Nearest Neighbour standard filter simply takes the nearest validated measurement to connect the map. The pipe will be regressed from the starting point to the possible ending point. The uncertainty of the starting point will be regressed to the ending point area. The two points are connected only when the Mahalanobis distance [42] (the distance measured based on correlations between variables

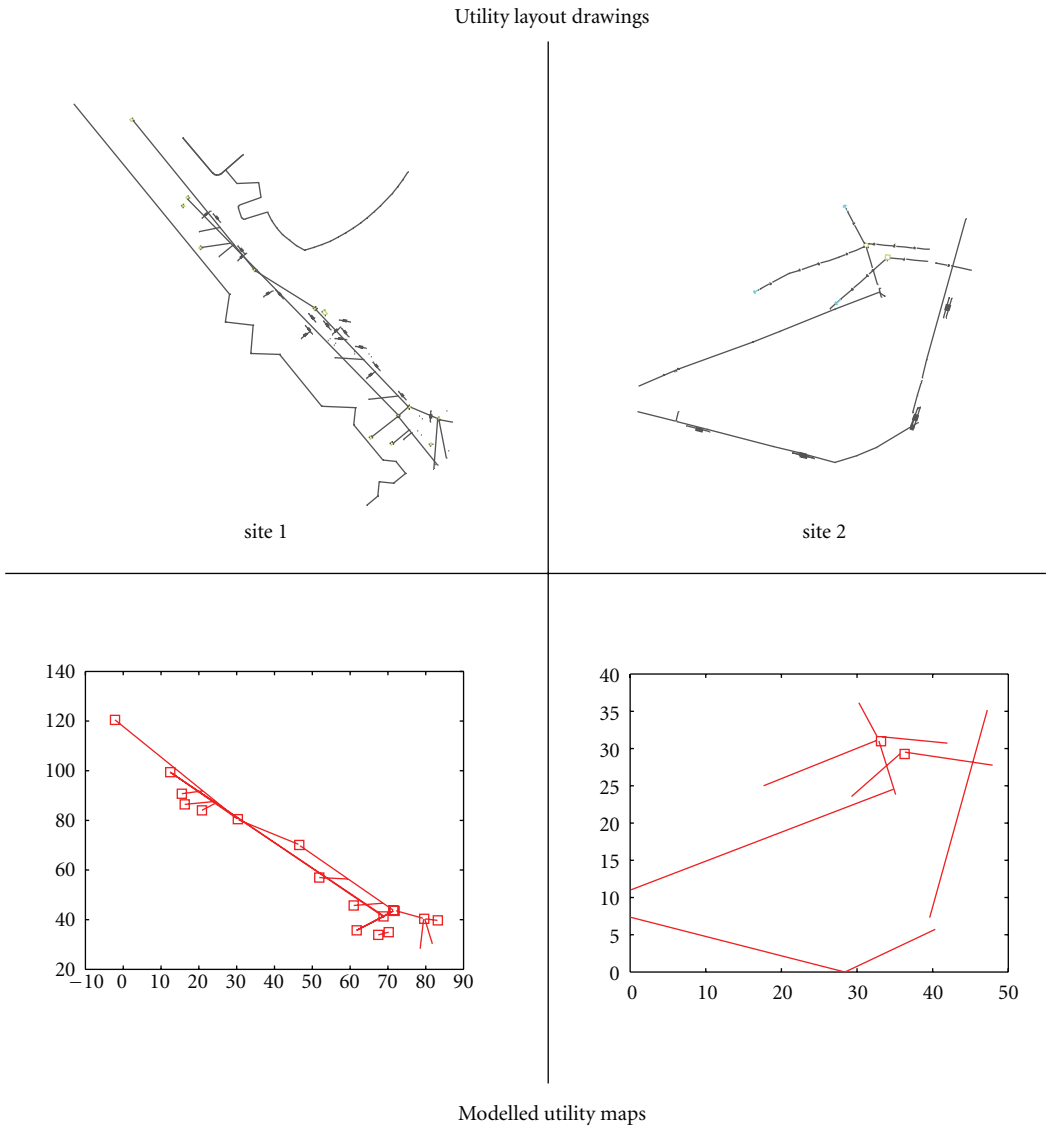

Figure 20: Utility maps for water utilities, (top) drawings from site survey, and (bottom) projections from modelling (created using JCBB) (images previously published in Chen and Cohn [41]).

by which different patterns can be identified and analysed) of two survey points (either manhole or GPR with pipe direction) is smaller than a threshold, that is, the validation gate. The validation gate is obtained from the inverse cumulative distribution at a significance level (typical values are 0.95 or 0.99; for this research 0.99 has been adopted as the significance level). The Nearest Neighbour algorithm uses individually compatible pairings to connect the maps, yet individually compatible pairings are not guaranteed to be jointly compatible to form a consistent hypothesis. Even if street observations and GPR analysis results are independent, correlations in the uncertainty of manhole locations might be present. *The JCBB method* addresses this issue by measuring the joint compatibility of a set of pairings and rejects spurious matching, thus is considered more robust in complex environments [43]. When dealing with the first manhole (where the GPR data and manhole location data are correlated), JCBB is preferable to Nearest Neighbour because the utilities entering the manhole often follow roughly similar directions and thus the uncertainties of these estimations are not independent. However, although JCBB is considered to be more accurate than the Nearest Neighbour method, it is more time consuming as it undertakes a relatively "global" search of the joint compatibility, controlled by the "branch and bound" method.

An experimental study was undertaken to assess the performance of the Nearest Neighbour and JCBB methods using site-based data, comprising a street survey and GPR survey for two sites (Figure 20). In each case the GPR is moved forward 3 m ($d = 3$ m) for each scan and the uncertainty was selected as 0.2 m for manhole location and 0.4 m for GPR point scans. In terms of uncertainty for pipe directions, 8° and 15° were selected for manhole observation and GPR scans, respectively (providing that the pipe direction could be identified using the approach outlined above), although if the GPR scans prove that the uncertainty selected was

inconsistent for part of the model then this uncertainty can be increased. JCBB and Nearest Neighbour were used to create the utility maps for both sites (Figure 20) and it is apparent that JCBB made three errors on the first site and none on the second, compared to eight errors and two errors for the two sites, respectively, using Nearest Neighbour. JCBB required 4.3 s and 2.1 s to produce the model for site one and two, respectively, compared to 0.06 s and 0.05 s for Nearest Neighbour for the same sites.

The data fusion algorithm proposed herein aims to fuse data from several different sensors and to generate a consistent and complete map. The proposed algorithm contributes to an important practical application by largely automating the process of generating utility maps from surveys by combining sensor data and street observations. Given the extent of invasive street works in most countries, this has considerable potential for application.

Future work will initially focus on further trials with real data and using actual utility records. Research will also be undertaken on the incorporation of data from other sensors such as vibro-acoustic and LFEM. Finally, although at present the system operates off line as a research prototype, the eventual goal is on-board operation, giving real-time mapping, and also the possibility of directing the operator to take further readings in the area of most uncertainty.

6. Conclusions

The MTU multisensor device project focuses not only on the development of the multisensor platform, but also intelligent combination of the sensors' outputs with information on the properties of the ground, via the development of a KBS, as well as utility companies' record data. It is widely reported that the deployment of a single geophysical sensing technology, or a sequential use of sensor technologies, is unlikely to locate all utilities in all but the simplest of utilities layouts and/or most favourable ground conditions. By fusing the datasets from the various sensors; by incorporating information on ground conditions to be encountered into the deployment strategy and assessing the ground conditions during the survey (thus understanding how the ground will influence the various sensing technologies); and by fusing the resultant data with existing utility records, the probability of being able to detect all utilities on a site will markedly increase.

The development of the sensing technologies has reached the stage where initial testing was undertaken and the findings provide important leads for those seeking to optimise individual sensor technologies or seeking to combine sensors to improve detection rates. The results from the three prototype sensing technologies proved very encouraging. Excitation of the water-filled pipe resulted in the detection and accurate plan location of the pipe using the prototype vibro-acoustic sensing technology, and significant potential was shown when the ground away from the pipe was excited. The prototype LFEM sensing technology detected anomalies that appear to correlate with those detected by the commercially available GPR, while the prototype PMF sensing technology located the position of the power cable crossing the site, that is, in the plane of cross-section, with a high degree of accuracy and confidence.

The KBS is under development, with research currently focused on developing correlations between geotechnical and geophysical properties of various soils and the changes in geophysical properties with the seasons and recent weather. The coaxial probe, developed to provide a means of direct measurement of the geophysical properties of the soil on site and thus inform the KBS of conditions on site, performed well and achieved values for the measured parameters that were close to the more traditional TDR approach. Research investigating the fusion of street survey and utility record data with GPR data to produce utility maps is producing encouraging results.

Acknowledgments

The authors wish to thank the UK Engineering and Physical Sciences Research Council for funding the project (EPSRC grants EP/F065965, EP/F06585X, EP/F065906, EP/F065973, EP/F06599X) and the project's many industrial partners who have contributed time, knowledge, and data to the project.

References

[1] W. McMahon, M. H. Burtwell, and M. Evans, "Minimising street works disruption: the real costs of street works to the utility industry and society," Tech. Rep. 05/WM/12/8, UK Water Industry Research, London, UK, 2005.

[2] T. Hao, H. J. Burd, D. J. Edwards, and C. J. Stevens, "Enhanced detection of buried assets," in *Proceedings of the Loughborough Antennas and Propagation Conference (LAPC '08)*, pp. 249–252, Loughborough, UK, March 2008.

[3] A. R. Beck, G. Fu, A. G. Cohn, B. Bennett, and J. G. Stell, "A framework for utility data integration in the UK," in *Proceedings of the Urban Data Management Society Symposium*, V. Coors, M. Rumor, E. M. Fendel, and S. Zlatanova, Eds., Stuttgart, Germany, October 2007.

[4] N. Metje, P. R. Atkins, M. J. Brennan et al., "Mapping the underworld: state of the art review," *Tunnelling and Underground Space Technology*, vol. 22, no. 5-6, pp. 568–586, 2007.

[5] A. C. D. Royal, C. D. F. Rogers, P. R. Atkins et al., "Mapping the underworld: location phase II—latest developments," in *Proceedings of the 28th International No-Dig 2010 Conference and Exhibition*, Singapore, November 2010.

[6] Q. Zhang, S. Pennock, M. Redfern, and A. Naji, "A novel OFDM based ground penetrating radar," in *Proceedings of the 13th Internarional Conference on Ground Penetrating Radar (GPR '10)*, Lecce, Italy, June 2010.

[7] J. M. Muggleton and M. J. Brennan, "The use of acoustic methods to detect & locate underground piping systems," in *Proceedings of the 9th International Conference on Recent Advances in Structural Dynamics (RASD '06)*, Southampton, UK, July 2006, paper no. WIP 3.

[8] J. M. Muggleton and M. J. Brennan, "The design and instrumentation of an experimental rig to investigate acoustic methods for the detection and location of underground piping systems," *Applied Acoustics*, vol. 69, no. 11, pp. 1101–1107, 2008.

[9] J. M. Muggleton, M. J. Brennan, and R. J. Pinnington, "Wavenumber prediction of waves in buried pipes for water leak detection," *Journal of Sound and Vibration*, vol. 249, no. 5, pp. 939–954, 2002.

[10] J. M. Muggleton, M. J. Brennan, and P. W. Linford, "Axisymmetric wave propagation in fluid-filled pipes: wavenumber measurements in in vacuo and buried pipes," *Journal of Sound and Vibration*, vol. 270, no. 1-2, pp. 171–190, 2004.

[11] J. M. Muggleton and M. J. Brennan, "Leak noise propagation and attenuation in submerged plastic water pipes," *Journal of Sound and Vibration*, vol. 278, no. 3, pp. 527–537, 2004.

[12] Y. Gao, M. J. Brennan, and P. F. Joseph, "A comparison of time delay estimators for the detection of leak noise signals in plastic water distribution pipes," *Journal of Sound and Vibration*, vol. 292, no. 3–5, pp. 552–570, 2006.

[13] O. Kuras, D. Beamish, P. I. Meldrum, and R. D. Ogilvy, "Fundamentals of the capacitive resistivity technique," *Geophysics*, vol. 71, no. 3, pp. G135–G152, 2006.

[14] O. Kuras, P. I. Meldrum, D. Beamish, R. D. Ogilvy, and D. Lala, "Capacitive resistivity imaging with towed arrays," *Journal of Environmental and Engineering Geophysics*, vol. 12, no. 3, pp. 267–279, 2007.

[15] A. Samouëlian, I. Cousin, A. Tabbagh, A. Bruand, and G. Richard, "Electrical resistivity survey in soil science: a review," *Soil and Tillage Research*, vol. 83, no. 2, pp. 173–193, 2005.

[16] H. Shima, S. Sakashita, and T. Kobayashi, "Developments of non-contact data acquisition techniques in electrical and electromagnetic explorations," *Journal of Applied Geophysics*, vol. 35, no. 2-3, pp. 167–173, 1996.

[17] V. M. Timofeev, *The employment of capacitively-coupled sensors in engineering and geological studies*, Ph.D. thesis, University of Moscow, Moscow, Russia, 1974.

[18] K. Y. Foo, P. R. Atkins, A. M. Thomas, and C. D. F. Rogers, "Capacitive-coupled electric-field sensing for urban sub-surface mapping: motivations and practical challenges," in *Proceedings of the 1st International Conference on Frontiers in Shallow Subsurface Technology (FSST '10)*, pp. 157–160, The Netherlands, January 2010.

[19] R. J. Pinnington and A. R. Briscoe, "Externally applied sensor for axisymmetric waves in a fluid filled pipe," *Journal of Sound and Vibration*, vol. 173, no. 4, pp. 503–516, 1994.

[20] B. Papandreou, E. Rustighi, and M. J. Brennan, "On the detection of shallow buried objects using seismic wave reflections," in *Proceedings of the 16th International Congress on Sound and Vibration (ICSV '09)*, p. 8, Krakow, Poland, July 2009, paper no. 101.

[21] B. Papandreou, M. J. Brennan, and E. Rustighi, "On the detection of objects buried at a shallow depth using seismic wave reflections," *Journal of the Acoustical Society of America*, vol. 129, no. 3, pp. 1366–1374, 2011.

[22] S. Self and D. Entwisle, "The structure and operation of the BGS National Geotechnical Properties Database," Internal Report IR/06/092, British Geological Survey, 2006.

[23] G. Curioni, D. N. Chapman, N. Metje et al., "Soil water content gradients with seasonal variations," in *Proceedings of the 3rd International Symposium on Soil Water Measurement Using Capacitance, Impedance and Time Domain Transmission*, Murcia, Spain, April 2010.

[24] C. D. F. Rogers, D. N. Chapman, D. Entwisle et al., "Predictive mapping of soil geophysical properties for GPR utility location surveys," in *Proceedings of the 5th International Workshop on Advanced Ground Penetrating Radar (IWAGPR '09)*, pp. 60–67, Granada, Spain, May 2009.

[25] A. M. Thomas, N. Metje, C. D. F. Rogers, and D. N. Chapman, "Ground Penetrating Radar interpretation as a function of soil response complexity in utility mapping," in *Proceedings of the 11th International Conference on Ground Penetrating Radar (GPR '06)*, Columbus, Ohio, USA, June 2006.

[26] A. M. Thomas, D. N. Chapman, C. D. F. Rogers, N. Metje, P. R. Atkins, and H. M. Lim, "Broadband apparent permittivity measurement in dispersive soils using quarter-wavelength analysis," *Soil Science Society of America Journal*, vol. 72, no. 5, pp. 1401–1409, 2008.

[27] A. M. Thomas, D. N. Chapman, C. D. F. Rogers, and N. Metje, "Electromagnetic properties of the ground: part I—fine-grained soils at the liquid limit," *Tunnelling and Underground Space Technology*, vol. 25, no. 6, pp. 714–722, 2010.

[28] A. M. Thomas, D. N. Chapman, C. D. F. Rogers, and N. Metje, "Electromagnetic properties of the ground: part II—the properties of two selected fine-grained soils," *Tunnelling and Underground Space Technology*, vol. 25, no. 6, pp. 723–730, 2010.

[29] R. L. van Dam, B. Borchers, and J. M. H. Hendrickx, "Methods for prediction of soil dielectric properties: a review," in *Detection and Remediation Technologies for Mines and Minelike Targets X*, vol. 5794 of *Proceedings of the SPIE*, pp. 188–197, Orlando, Fla, USA, 2005.

[30] N. R. Peplinski, F. T. Ulaby, and M. C. Dobson, "Dielectric properties of soils in the 0.3-1.3 GHz range," *IEEE Transactions on Geoscience and Remote Sensing*, vol. 33, no. 3, pp. 803–807, 1995.

[31] V. L. Mironov, L. G. Kosolapova, and S. V. Fomin, "Physically and mineralogically based spectroscopic dielectric model for moist soils," *IEEE Transactions on Geoscience and Remote Sensing*, vol. 47, no. 7, Article ID 4895263, pp. 2059–2070, 2009.

[32] M. C. Dobson, F. T. Ulaby, M. T. Hallikainen, and M. A. El-Rayes, "Microwave dielectric behavior of wet soil-part II: dielectric mixing models," *IEEE Transactions on Geoscience and Remote Sensing*, vol. GE-23, no. 1, pp. 35–46, 1985.

[33] G. C. Topp, J. L. Davis, and A. P. Annan, "Electromagnetic determination of soil water content: measurements in coaxial transmission lines," *Water Resources Research*, vol. 16, no. 3, pp. 574–582, 1980.

[34] K. E. Saxton, W. J. Rawls, J. S. Romberger, and R. I. Papendick, "Estimating generalized soil-water characteristics from texture," *Transactions of the ASAE*, vol. 50, no. 4, pp. 1031–1036, 1986.

[35] K. E. Saxton and W. J. Rawls, "Soil water characteristic estimates by texture and organic matter for hydrologic solutions," *Soil Science Society of America Journal*, vol. 70, no. 5, pp. 1569–1578, 2006.

[36] D. J. Daniels, *Ground Penetrating Radar*, The Institution of Engineering and Technology, London, UK, 2nd edition, 2004.

[37] D. A. Robinson, S. B. Jones, J. M. Wraith, D. Or, and S. P. Friedman, "A review of advances in dielectric and electrical conductivity measurement in soils using time domain reflectometry," *Vadose Zone Journal*, vol. 2, pp. 444–475, 2003.

[38] U. Kaatze, "Techniques for measuring the microwave dielectric properties of materials," *Metrologia*, vol. 47, no. 2, pp. S91–S113, 2010.

[39] H. Durrant-Whyte and T. Bailey, "Simultaneous localization and mapping: part I," *IEEE Robotics & Automation Magazine*, vol. 13, no. 2, pp. 99–110, 2006.

[40] W. E. L. Grimson, *Object Recognition by Computer: The Role of Geometric Constraints*, MIT Press, Cambridge, UK, 1990.

[41] H. Chen and A. G. Cohn, "Probabilistic robust hyperbola mixture model for interpreting ground penetrating radar data," in *Proceedings of the IEEE World Congress on Computational Intelligence (WCCI '10)*, Barcelona, Spain, 2010.

[42] R. De Maesschalck, D. Jouan-Rimbaud, and D. L. Massart, "The mahalanobis distance," *Chemometrics and Intelligent Laboratory Systems*, vol. 50, no. 1, pp. 1–18, 2000.

[43] J. Neira and J. D. Tardós, "Data association in stochastic mapping using the joint compatibility test," *IEEE Transactions on Robotics and Automation*, vol. 17, no. 6, pp. 890–897, 2001.